Coastal Engineering 56 (2009) 543–558

Contents lists available at ScienceDirect

Coastal Engineering

journal homepage: www.elsevier.com/locate/coastaleng

# Numerical analysis of wave loads for coastal structure stability

Raul Guanche, Inigo J. Losada *, Javier L. Lara

*Environmental Hydraulics Institute "IH Cantabria", Universidad de Cantabria, E.T.S.I. de Caminos, Canales y Puertos. Avda. de los Castros s/n. 39005 Santander. Spain*

ARTICLE INFO

*Article history:*
Received 7 May 2008
Received in revised form 14 November 2008
Accepted 18 November 2008
Available online 20 January 2009

*Keywords:*
Coastal structures
Structure stability
Wave loads
Numerical model
Wave and structure interaction

ABSTRACT

The numerical model COBRAS-UC [Losada, I.J., Lara, J.L., Guanche,R., Gonzalez-Ondina, J.M. (2008). Numerical analysis of wave overtopping of rubble mound breakwaters. Coastal Engineering, Vol 55 (1), 47–62.] is used to carry out a two-dimensional analysis of wave induced loads on coastal structures. The model calculates pressure, forces and moments for two different cross-sections corresponding to a low-mound and a conventional rubble-mound breakwater with a crown-wall under regular and irregular incident wave conditions. Predicted results are compared with experimental information provided in Losada et al. [Losada, I.J., Lara, J.L., Guanche,R., Gonzalez-Ondina, J.M. (2008). Numerical analysis of wave overtopping of rubble mound breakwaters. Coastal Engineering, Vol 55 (1), 47–62.] and Lara et al. [Lara, J.L., Losada, I.J., Guanche, R. (2008). "Wave interaction with low mound breakwaters using a RANS model". Ocean engineering (35), pp 1388–1400; doi:10.1016/j.oceaneng.2008.05.006.] on a 1:20 scale. Good agreement is found, and the differences between both typologies are explained in detail. Additionally, numerical results are also compared with several semi-empirical formulae recommended for design at both the 1:20 model scale and two prototype cross-sections. Results suggest that COBRAS-UC is able to provide realistic stability information that can be used to complete the approach based on currently existing methods and tools.



## 1. Introduction

In an effort to provide guidelines for designing coastal structures, numerous physical model tests to evaluate structure stability have been performed. Formulae to estimate wave induced forces and moments have also been obtained. Most of these formulae are summarized in the Coastal Engineering Manual (CEM) (USACE, 2002) including recommendations regarding their range of application and limitations. These tools, together with a few wave theory-based stability analysis methods, have proven to be successful but as explained in CEM, their application is limited to a reduced number of typologies and incident wave conditions.

During the last decade, and in order to overcome some of these limitations, several numerical models have been developed based mainly on nonlinear shallow water equations (NSW) Brocchini and Dodd (2008), and more recently on Boussinesq (Engsig-Karup et al., 2008) or Navier–Stokes type models (Liu et al., 1999; Hsu et al., 2002; Hur & Mizutani 2003; Li et al., 2004). Different numerical techniques have been used to solve these sets of equations. Nevertheless, and independently of the structure typologies considered, the degree of validation and the accuracy of the results achieved by the different models vary. Most of them have been primarily applied to the prediction of hydraulic response design parameters associated to wave reflection, transmission, run-up and overtopping. In an effort to complete the coastal structure design process, the possibility of applying numerical models to wave induced load analysis is worth exploring. A scarce amount of work can be found in the literature.

Here, a two-dimensional numerical model based on the Volume-Averaged Reynolds-Averaged Navier–Stokes equations (VARANS), called COBRAS-UC (Losada et al., 2008), is used to carry out a wave induced load analysis at laboratory and prototype scales. In order to evaluate the model performance under different conditions, two structure typologies with different hydraulic responses have been selected; a low-mound breakwater with a response dominated by wave reflection, and a conventional rubble-mound breakwater with a crown wall in which the hydraulic response results from the combination of wave run-up and breaking on the breakwater slope, and wave transmission through the rubble-mound layers.

The model applicability to wave induced load analysis is evaluated in four phases: (1) pressure time series is calculated at different locations, and representative pressure statistic parameters are validated against data sets obtained on a 1:20 physical model carried out at the University of Cantabria wave flume for both regular and irregular waves; (2) a validation of wave forces and moments acting on the structure is carried out; (3) the numerical and semi-empirical formulae predictions at laboratory scale are compared and (4) the model is applied to prototype cross-sections, and results are compared with semi-empirical formulae.

These four phases are the core of the paper. Finally, some conclusions and a discussion are presented.

* Corresponding author.
*E-mail address:* losadai@unican.es (I.J. Losada).

0378-3839/$ – see front matter © 2008 Elsevier B.V. All rights reserved.
doi:10.1016/j.coastaleng.2008.11.003

## 2. Description of the numerical model

COBRAS-UC (Losada et al., 2008) solves the 2DV Reynolds Average Navier–Stokes (RANS) equations, based on the decomposition of the instantaneous velocity and pressure fields, into mean, and turbulent components, and the $k$–$\varepsilon$ equations for the turbulent kinetic energy ($k$), and the turbulent dissipation rate ($\varepsilon$). The influence of turbulence fluctuations on the mean flow field is represented by the Reynolds stresses. The governing equations for $k$–$\varepsilon$ are derived from the Navier–Stokes equations, and higher order correlations of turbulence fluctuations in $k$ and $\varepsilon$ equations are replaced by closure conditions. A nonlinear algebraic Reynolds stress model is used to relate the Reynolds stress tensor and the strain rate of mean flow. The free surface movement is tracked by the Volume of Fluid (VOF) method. The flow inside the porous media is solved through the resolution of the Volume-Averaged Reynolds Averaged Navier–Stokes (VARANS) equations; see Liu et al. (1999) and Hsu et al. (2002) for the complete mathematical formulation. These equations are derived by integrating the RANS equations over a control volume. In the VARANS equations, the interfacial forces between the fluid and solids have been modeled according to the extended Forchheimer relationship, in which both linear and nonlinear drag forces are

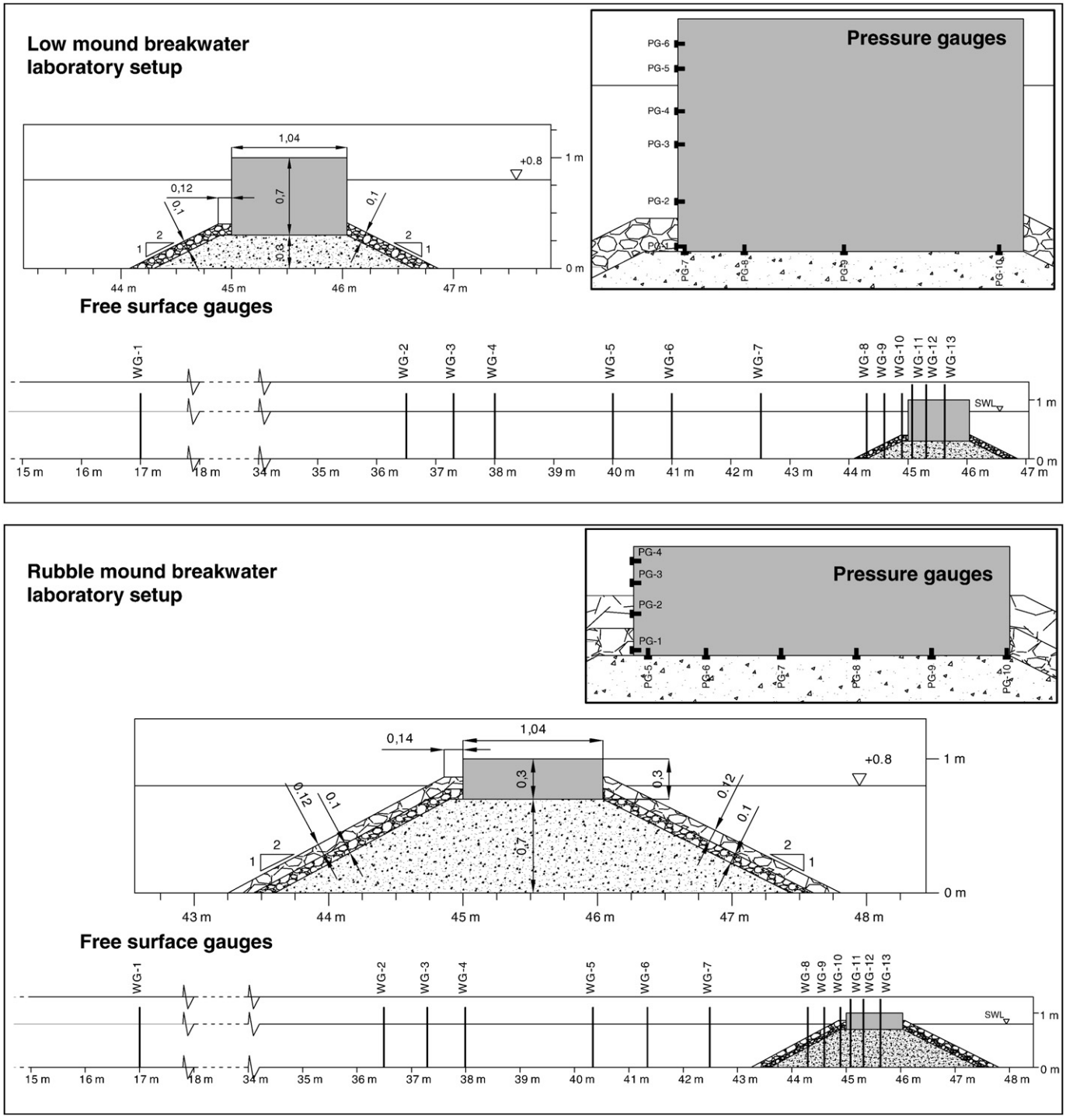


**Fig. 1.** Experimental set-up (pressure and free surface gauges) for the low-mound and rubble-mound breakwater cross-sections.

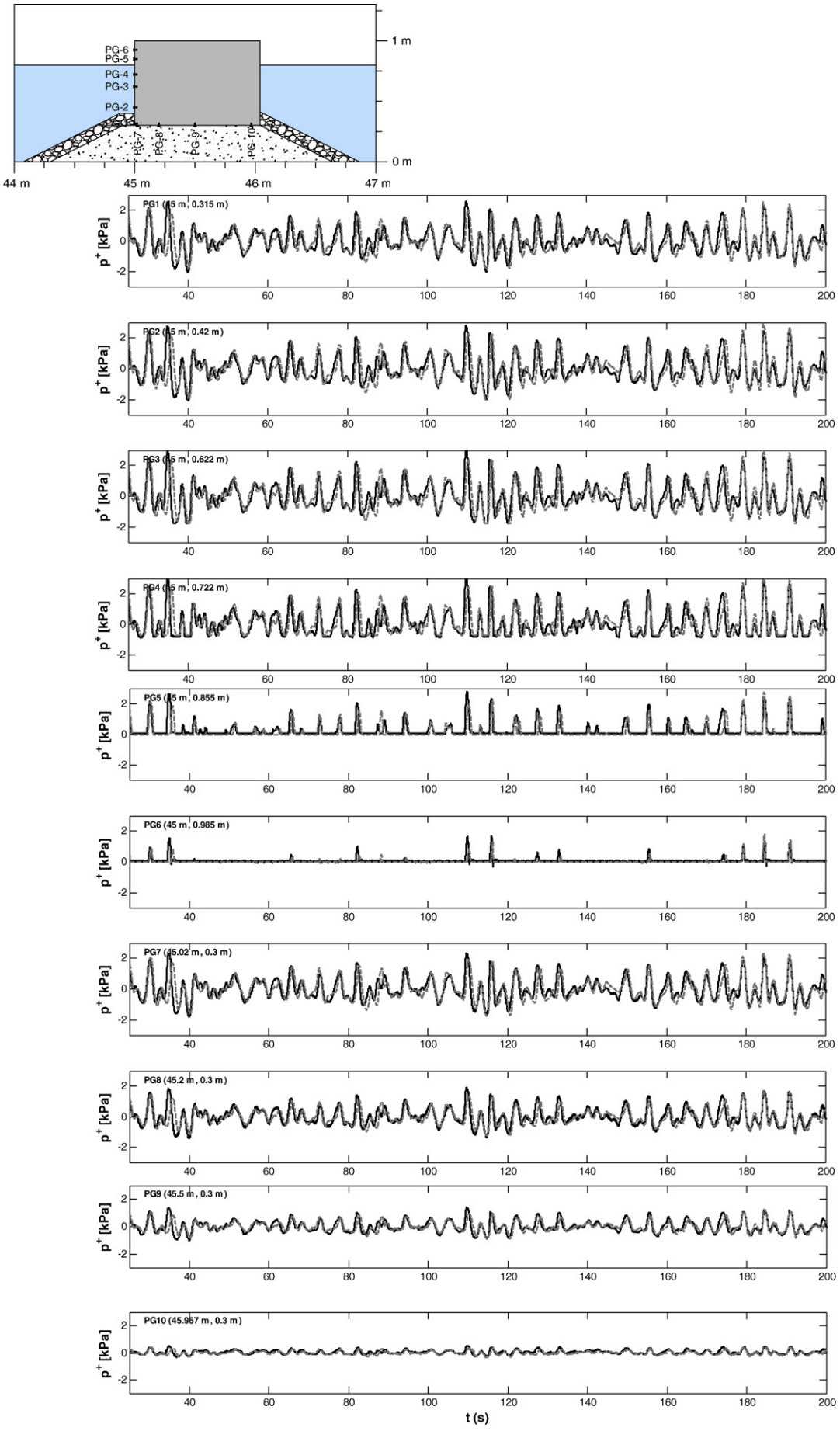


**Fig. 2.** Pressure time series for the low mound breakwater. Solid line: laboratory measurements. Dashed line: numerical results. Case: $H_s = 0.18$ m $T_p = 6$ s.

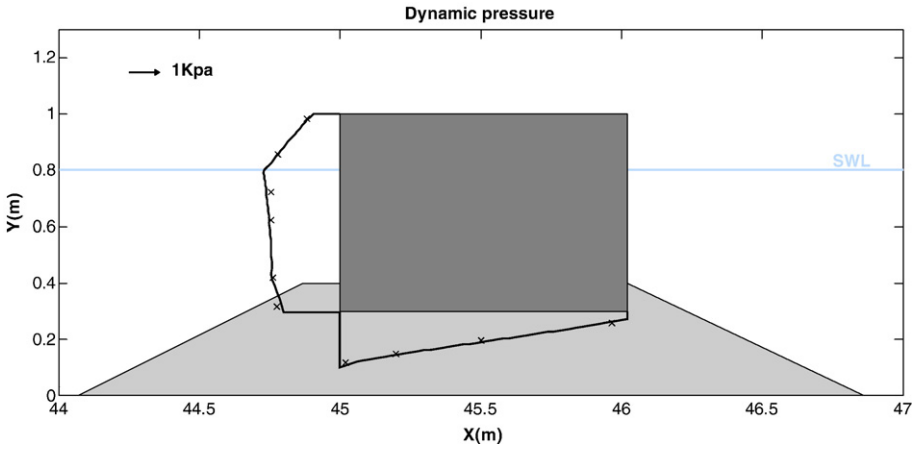


**Fig. 3.** Distribution of wave pressure on the low-mound breakwater for the maximum wave induced horizontal force event. Cross symbol: laboratory measurements, solid line: numerical results. Case: $H_s = 0.21$ m $T_p = 3$ s.

included in the equations. The linear and nonlinear terms in this relationship depend on $\alpha$ and $\beta$, the only two empirical parameters used in the calibration of the numerical model, and the porosity, $n$. An additional parameter affecting the inertia term is included in the formulation to take into account the added mass. The model has been under a continuous development process based on an extensive validation procedure, carried out for low-crested structures (Garcia et al., 2004, Losada et al., 2005; Lara et al., 2006a), wave breaking on permeable slopes (Lara et al., 2006b), surf zone hydrodynamics on natural beaches (Torres-Freyermuth et al., 2007) and overtopping on rubble mound breakwaters and low-mound breakwaters (Losada et al., 2008; Lara et al., 2008). Further details on the numerical model, the calibration process and recommended values for the porous flow equation can be found in these references.

## 3. Benchmark experiments for structural stability

In order to guarantee suitable benchmark cases to inspect the model performance, a set of experiments has been carried out. The experimental tests consisted of two sets of flume experiments on a 1:20 physical model in which regular and irregular waves encountered a low-mound and a rubble-mound breakwater with a crown-wall, respectively. An extensive monitoring set-up including free surface, pressure and overtopping discharge has been considered. In Fig. 1, a sketch of the geometry, including the position of the free surface and pressure gauges used in this exercise is presented for both the low-mound and the rubble-mound cross-sections. More details on the experimental set-up, wave flume dimensions, target wave conditions, sampling frequency, and experimental hydraulic response, etc. can be found in Losada et al. (2008) for the rubble-mound breakwater and in Lara et al. (2008) for the low-mound breakwater.

## 4. Numerical analysis of wave induced loads

As explained in the introduction, COBRAS-UC ability to address the wave induced loads is presented in four different phases. The first one, which includes numerically calculated pressure, is presented next.

### 4.1. Pressure validation

An extensive pressure validation procedure has been carried out by comparing measured pressure time series at different gauges, the dynamic pressure distribution around the structures and several pressure statistic parameters with the equivalent predictions made by COBRAS-UC.

In Fig. 2 we present a comparison of the measured and predicted dynamic pressure time series for an irregular wave case ($H_s = 0.18$ m $T_p = 6$ s) at the low-mound breakwater cross-section. The comparison includes six pressure gauges along the vertical face of the caisson (PG1 to PG6) and four additional gauges underneath the caisson (PG7 to PG10). The solid line represents the laboratory measurements while the dashed line represents the numerical solution.

The numerical solution was obtained on a grid covering the complete wave flume with a total number of 2325 cells in the $x$-direction and 92 cells in the $y$-direction. A variable cell resolution was used in the grid, with a 5 cm cell size in the $x$-direction of the wave generation region, increasing resolution up to 2 cm in the vicinity of the breakwaters. In the $y$-direction, 1 cm and 3 cm cell sizes have been used above and under the SWL, respectively.

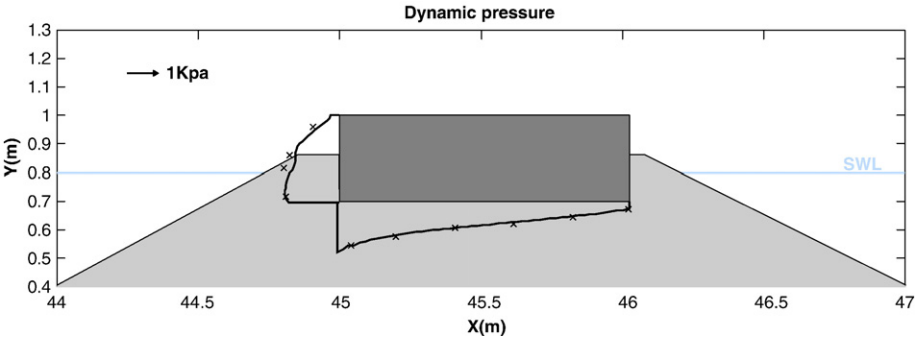


**Fig. 4.** Distribution of wave pressure on a rubble-mound breakwater for the maximum wave induced horizontal force event. Cross symbol: laboratory measurements, solid line: numerical results. Case: $H_s = 0.15$ m $T_p = 3$ s.

The criteria to choose linear ($\alpha$) and non-linear ($\beta$) drag parameters is the same as the one followed in Losada et al. (2008) and Lara et al. (2008). The best-fit values for $\alpha$ and $\beta$ were evaluated by comparing experimental data and numerical results of free surface and pressure time series for two regular wave cases ($H=0.1$ m and $T=3$ s; $H=0.1$ m and $T=5$ s) for both configurations. After a trial and error process, the best-fit parameter calculated values for the conventional rubble-mound breakwater were $\alpha=200$ and $\beta=0.8$ for the breakwater core; $\alpha=200$ and $\beta=1.1$ for the small gravel external layer and $\alpha=200$ and $\beta=0.7$ for the large gravel external layer. The values for the low-mound breakwater were $\alpha=200$ and $\beta=0.8$ for the breakwater core and $\alpha=200$ and $\beta=1.1$ for the external layer. Additional information regarding sensitivity analysis and numerical wave generation can be found in Losada et al. (2008) and Lara et al. (2008). The model was run for 48 h, simulating 650 s and, on average, 100 waves.

In general, the model is able to predict the pressure time series accurately at every location. The time series agree for larger and smaller waves. The model is able to predict the chopped troughs visible in the wave gauges above the still water level where the predicted results are highly dependent on the predicted run-up water lens. Overall, only minor discrepancies in height and phase are shown for a few waves along the time series. Moreover, the numerical model predicts well the pressure time series underneath the caisson (P7–P10). The accurate prediction of the damping induced as waves propagate underneath the caisson towards the leeward side of the structure indicates that the modelling of wave transmission through the porous media is well solved.

In Figs. 3 and 4 the distribution of wave pressure on the caisson of the low-mound breakwater and on the crown-wall of the rubble-mound breakwater are presented. Wave pressure distribution is plotted for the instant of maximum horizontal force.

For the low-mound breakwater case, the model predicts maximum pressure at the SWL as suggested in Goda (1985). The uplift pressure distribution acting on the bottom of the caisson has a trapezoidal shape due to a non-zero heel pressure induced by wave transmission (Losada et al., 1993).

For the rubble-mound breakwater, Fig. 4, the model predicts an almost trapezoidal pressure distribution law at the front face of the crown-wall as a result of the combination of pulsating loads and wave overtopping ($q=0.0007$ m$^3$/m/s) as suggested by Martín et al. (1999). The effect of the rubble-mound layer on the pressure distribution is also clearly visible. The uplift pressure distribution is also trapezoidal for this case.

Comparison with experimental data is satisfactory for both cross-sections. Small discrepancies are evident for the rubble-mound case which is far more difficult to model since reflection; run-up and overtopping are dominated by the wave breaking process on the breakwater rubble-mound layers, therefore affecting the prediction of pressure distribution. Moreover, the influence of the individual stone geometry of the outer layer, which has not been considered in the numerical simulations, is clearly affecting the pressure distribution at the outer layer berm, where the model is not able to reproduce the experimentally recorded values as well as in other locations.

Since wave induced loads analysis requires accurate quantitative pressure estimates, COBRAS-UC is verified against the experimental

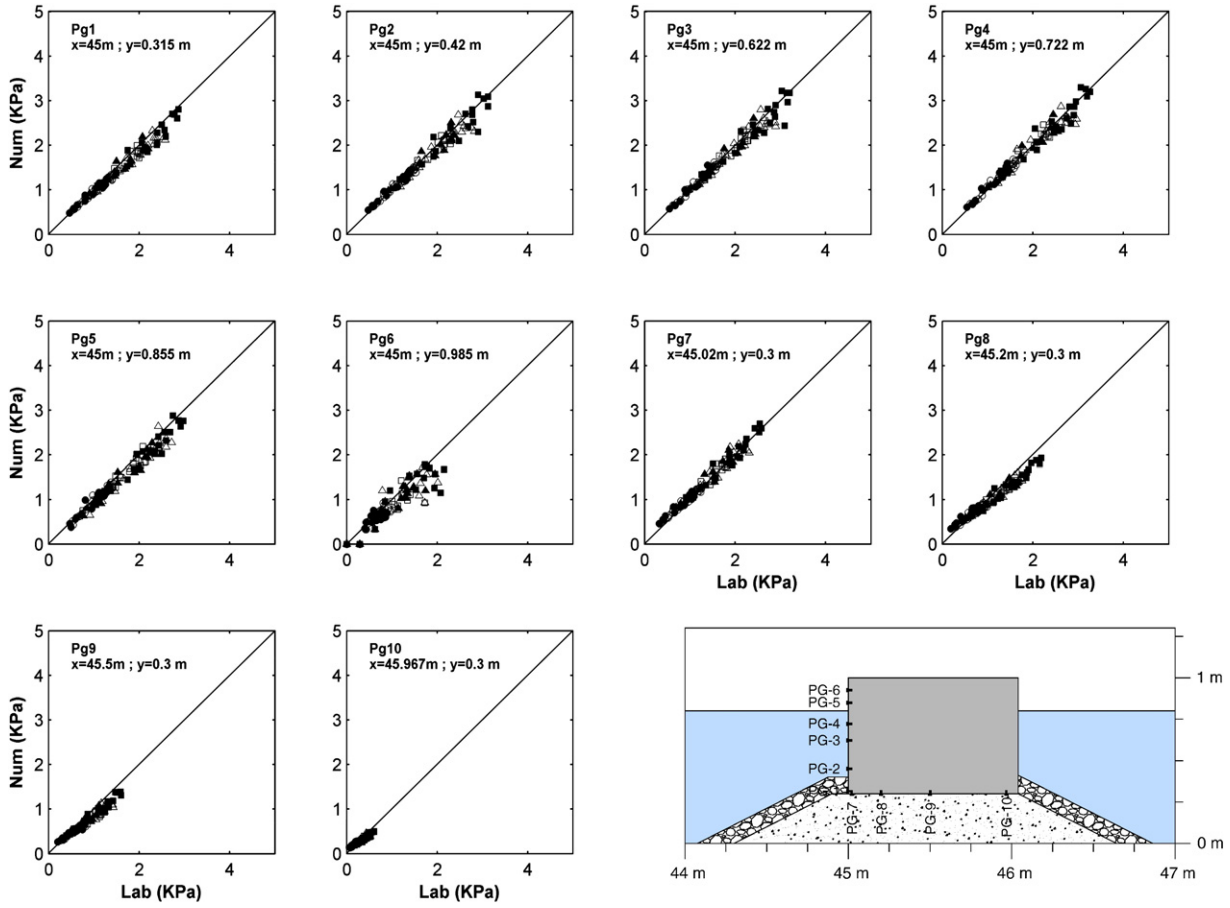


**Fig. 5.** Low-mound breakwater. Comparison of predicted and measured pressure related statistic parameters: ● Mean ○ Root-Mean-Square. ■ Maximum □ (q85%). ▲ (q90%). ▼ (q95%). All the irregular tests are included.

**Table 1**

| Positive pressure statistics: irregular waves. | | | | |
|---|---|---|---|---|
| | Low-mound breakwater | | Rubble-mound breakwater | |
| | Mean error | Standard deviation | Mean error | Standard deviation |
| Mean pressure | 2.06% | ±17.70% | 10.26% | ±31.64% |
| Rms pressure | −2.90% | ±12.45% | 2.56% | ±24.48% |
| Pressure ($q_{85\%}$) | −5.69% | ±12.67% | −2.74% | ±21.23% |
| Pressure ($q_{90\%}$) | −6.55% | ±12.21% | −4.16% | ±19.55% |
| Pressure ($q_{95\%}$) | −7.65% | ±13.35% | −6.32% | ±18.99% |
| Pressure max | −7.09% | ±12.68% | −9.33% | ±27.23% |

results for both geometries, regular and irregular waves, by comparing the mean of the positive (inshore directed) pressure values. The mean relative errors are calculated as the difference between predicted and experimental values, divided by the experimental value.

$$\text{error}(\%) = \frac{\phi_{\text{predicted}} - \phi_{\text{measured}}}{\phi_{\text{measured}}} \cdot 100$$

Errors, expressed in percentages, are calculated for each of the pressure gauges; negative values represent an under prediction by COBRAS-UC.

Regular wave show similar errors for all pressure gauges. For the low-mound breakwater, the mean relative error including all the gauges, is −6.11%, indicating a good accuracy and a slight under prediction. The standard deviation calculated is ±14.99%.

For the rubble-mound breakwater cross-section the comparison for regular wave simulations gives a −9.29% error, which is still a good result, but the standard deviation increases to ±39.66%. As said, the accurate modelling of the rubble-mound breakwater case is far more difficult due to the processes involved, but results show that this is also done reasonably well for engineering purposes. There are several reasons that could explain what the discrepancies are due to. The rough slope induces an important wave deformation before breaking that may end in broken wave induced loads. The influence of the rubble mound slope deviations from the originally modelled profile on the wave deformation, which is not considered in the numerical setup, is also another possible source of discrepancy.

A similar behaviour can be found when irregular test cases are considered. Since irregular incident waves represent a more realistic case, detailed information is provided. COBRAS-UC quantitative accuracy is tested by verifying both the following measured and predicted statistic parameters: mean, root mean square, maximum and three quantiles (85%, 90% and 95%).

In Fig. 5 comparisons between predicted and measured values are shown for the low-mound breakwater cross-section.

The 10 pressure gauges are included in order to show how sensitive predictions are to the gauge location. Axis scales are kept constant in order to better represent the pressure magnitude at the different gauge locations around the caisson. Numerical values are shown in Table 1. COBRAS-UC shows a similar performance for all pressure gauges. As expected, gauge 6, located at the top of the caisson, presents a higher standard deviation. At this position, pressure results are highly sensitive to free surface and overtopping prediction quality. Figures listed in Table 1 indicate that maximum values and quantiles show larger errors than the mean and the root-mean-square. Highest pressure records are due to highest waves which are usually associated with important overtopping events.

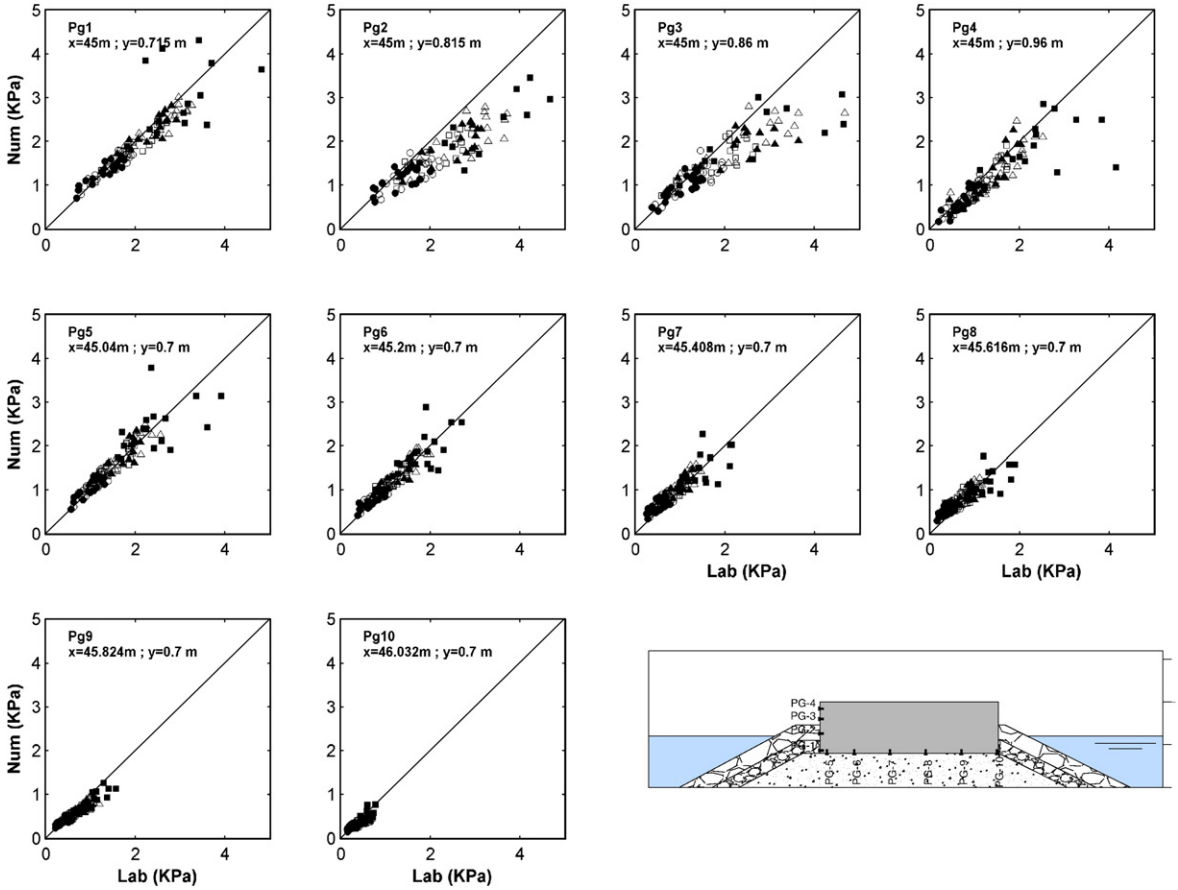


**Fig. 6.** Rubble-mound breakwater. Comparison of predicted and measured pressure related statistic parameters: ● Mean ○ Root-Mean-Square. ■ Maximum □ (q85%). ▲ (q90%). ▼ (q95%). All the irregular tests are included.

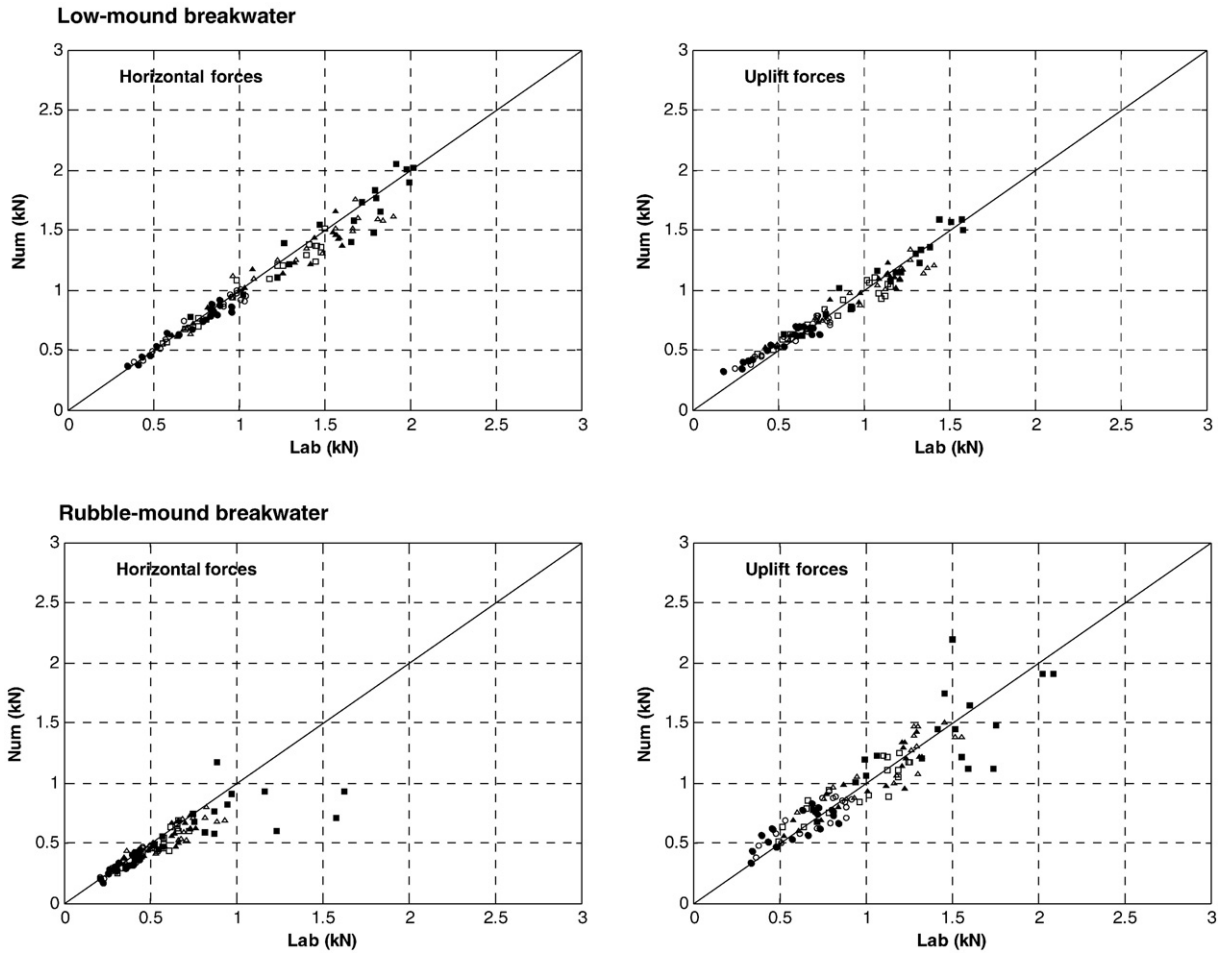


**Fig. 7.** Comparison of predicted and experimental force related statistic parameters. Irregular waves. Low- (top panel) and rubble-mound (lower panel) breakwaters ● Mean ○ Root Mean Square. ■ Maximum □ (q85%). ▲ (q90%). ▼ (q95%).

Nevertheless, the calculated relative error varies from 2% to 7%, considered very satisfactory. The standard deviation is in the range of 12% with a maximum of 17% for the mean. In Fig. 6 results are presented for the rubble-mound breakwater cross-section. Relative errors and standard deviations are listed in Table 1.

As expected, at the front face of the crown-wall, gauges 2 and 3, COBRAS-UC shows a significant scattering and a consistent trend of under-predicting experimental results. The highest scattering is calculated for gauge 3, located very close to the still water level and just above the rubble mound. As previously mentioned, the outer layer irregularity, not considered in the numerical model geometry, causes these discrepancies. The maximum pressure event is due to larger waves. Because of this the model under predicts the maximum pressure. Underneath the caisson wave impulse is reduced due to damping by the rubble-mound and the core material. Consequently, pressure results underneath the caisson are less scattered. Still, comparisons are very satisfactory with relative errors below 10%.

Results obtained are encouraging to proceed to phase two, which aims to verify COBRAS-UC performance against forces and moments acting on the structure as a basis for stability analysis.

### 4.2. Forces and moments validation

The caisson and crown-wall stability depend mainly on the resultant forces and moments acting on them. In this section, the forces and moments resulting from the integration of the validated pressure distribution are compared against the forces and moments calculated from the physical model tests.

In our approach, the wave induced horizontal forces are obtained by integrating numerical and experimental pressure distributions on

**Table 2**

Positive force statistics: irregular waves.

| | Low-mound breakwater | | | | Rubble-mound breakwater | | | |
|---|---|---|---|---|---|---|---|---|
| Force | Horizontal | | Uplift | | Horizontal | | Uplift | |
| Statistic | Mean error | Standard deviation | Mean error | Standard deviation | Mean error | Standard deviation | Mean error | Standard deviation |
| Mean force | −2.45% | ±6.22% | 7.67% | ±11.31% | −5.76% | ±9.49% | 5.81% | ±18.22% |
| RMS force | −2.82% | ±5.26% | 2.59% | ±7.93% | −7.82% | ±8.23% | 3.94% | ±15.64% |
| Force ($q_{85\%}$) | −4.13% | ±5.57% | −1.36% | ±9.41% | −9.22% | ±9.87% | 1.66% | ±13.95% |
| Force ($q_{90\%}$) | −4.36% | ±6.49% | −1.90% | ±7.95% | −10.17% | ±10.29% | 1.22% | ±11.80% |
| Force ($q_{95\%}$) | −5.47% | ±7.62% | −3.56% | ±7.70% | −12.72% | ±11.93% | 1.60% | ±12.23% |
| Force max | −2.83% | ±7.79% | −0.64% | ±7.41% | −18.15% | ±19.91% | −0.64% | ±19.50% |

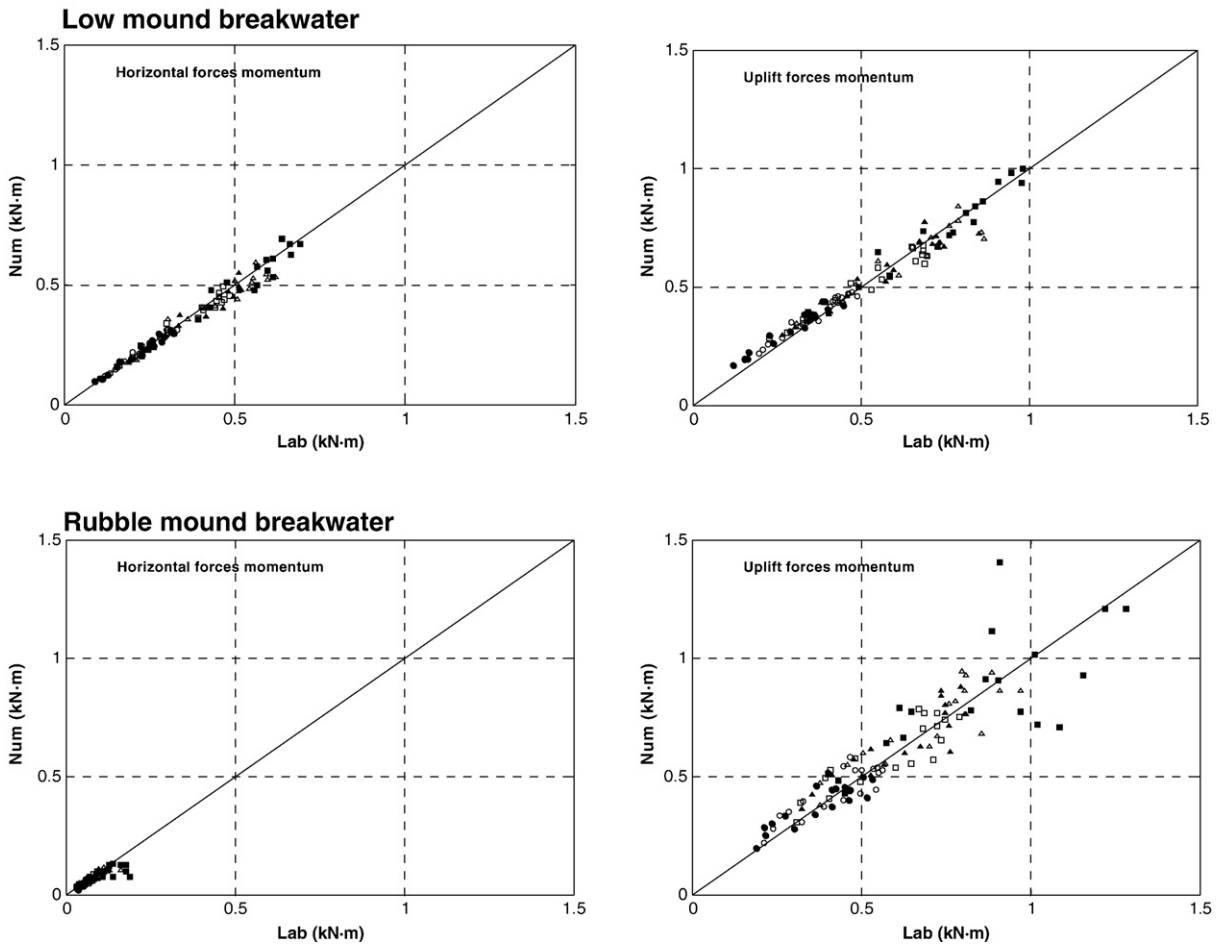


**Fig. 8.** Comparison of predicted and experimental momentum related statistic parameters. Irregular waves. Low-(top panel) and rubble-mound (lower panel) breakwaters ● Mean ○ Root Mean Square. ■ Maximum □ (q85%). ▲ (q90%). ▼ (q95%).

the vertical face of the structure, while the uplift force results from integrating the pressure underneath the structure. Since laboratory pressure records have been taken using a limited number of gauges, a linear law has been fitted to the discrete pressure distributions.

In Fig. 7 and Table 2 we compare the experimental and predicted force parameters (mean, root mean square, maximum and quantiles) for both the low-mound and rubble-mound cross-sections. The comparison includes horizontal and vertical forces for all the irregular wave tests considered with and without overtopping.

For the low-mound cross-section, both the horizontal and uplift forces show a very good agreement, with small mean relative errors. In general, COBRAS-UC tends to under-predict the horizontal force, presenting a small overestimation for the mean vertical force. In this case the maximum horizontal and uplift forces are calculated with a very good agreement. It is also important to note that standard deviation is kept below ± 10% for both the horizontal and uplift forces.

As expected from the previous pressure analysis, results for the rubble-mound cross-section show a different degree of agreement than that obtained for the low-mound breakwater section. In general, the numerical model under-predicts horizontal forces, and the standard deviation is larger than that observed for the low-mound breakwater, but the errors in the prediction are still in a very reasonable range. Deviations in the horizontal force are due to the model's inaccurate prediction of the broken waves induced pressure. However, the model is able to predict uplift forces with a much higher accuracy, as can be seen in Table 2.

The experimental moments' statistics (mean, root-mean-square, maximum and quantiles) for both the low-mound and rubble-mound cross-sections are compared against the predicted values in Fig. 8 and Table 3.

Consistently with previous results, low-mound and rubble-mound breakwaters show a different performance, the best results being

**Table 3**

Positive momentum value statistics: irregular waves.

| | Low mound breakwater | | | | Rubble mound breakwater | | | |
|---|---|---|---|---|---|---|---|---|
| Momentum | Horizontal | | Uplift | | Horizontal | | Uplift | |
| Statistic | Mean error | Standard deviation | Mean error | Standard deviation | Mean error | Standard deviation | Mean error | Standard deviation |
| Mean momentum | −2.02% | ±5.00% | 12.94% | ±12.67% | −14.19% | ±12.03% | 3.54% | ±15.46% |
| RMS momentum | −2.85% | ±4.70% | 5.38% | ±8.10% | −14.56% | ±9.76% | 3.20% | ±14.12% |
| Momentum ($q_{85\%}$) | −2.44% | ±5.92% | 0.70% | ±8.98% | −16.24% | ±10.42% | 1.60% | ±13.90% |
| Momentum ($q_{90\%}$) | −4.53% | ±6.34% | 0.23% | ±7.72% | −14.71% | ±12.46% | 2.98% | ±11.58% |
| Momentum ($q_{95\%}$) | −5.53% | ±7.88% | −2.58% | ±8.79% | −17.46% | ±8.39% | 3.03% | ±12.57% |
| Momentum max | −2.94% | ±7.79% | −0.29% | ±7.52% | −21.33% | ±17.34% | 0.20% | ±20.66% |

**Table 4**
Comparison with semi empirical formulations — low mound breakwater.

| Model | Mean error | Standard deviation |
|---|---|---|
| COBRAS-UC | −2.38% | ±7.06% |
| Linear theory | −19.26% | ±18.52% |
| Sainflou (1928) | −5.66% | ±22.77% |
| Nagai (1973) | 4.25% | ±22.79% |
| Takahashi et al. (1994) | 2.88% | ±23.35% |

achieved for the first one. Results show a similar standard deviation, lower than ±10%. Similar errors are found for the higher moment statistics. However, it should be noted that larger errors are found for the mean vertical moment. We believe that this is due to the influence of smaller events, in which slight deviations in absolute terms induce high relative errors. Finally, the model is able to capture with good accuracy the maximum horizontal and vertical moments, with errors and standard deviations lower than 5% and 10%, respectively.

Regarding the rubble-mound breakwater, note that the model shows a poorer performance. The prediction of the vertical moment by COBRAS-UC is very good, with relative errors in the range of 3%. However, the standard deviation has increased. The quality of the agreement found for the horizontal moments is not as good, since mean relative errors increase up to 21% for the maximum moment. Note that the maximum horizontal pressure event was not accurately solved. Still, the order of the errors found can be considered to be acceptable.

## 5. Comparison with semi-empirical formulae

Wave generated pressure distributions and corresponding forces and moments are non trivial functions of incident wave conditions, structure typology and geometry. This is especially certain for crown-walls, where the load on the concrete cap occurs only if the run-up reaches the wall, run-up being highly dependent on the porous characteristics of the seaward face of the structure.

For several decades, semi-empirical formulae for estimating pressure distribution, forces and moments based on small-scale model tests have been, together with direct physical modelling, the only available resources for stability analysis. A long list of formulae and methods based on wave theories can be found in the CEM (USACE, 2002). Sainflou (1928), for impermeable vertical walls under standing wave conditions, is one of the oldest formulations. Most of the other formulae available for impermeable vertical or inclined walls are based on the pioneering method presented by Goda (1974).

In this work, results for comparison with the numerical model have been obtained considering four different methods: Linear theory, Sainflou (1928), Nagai (1973) and Takahashi et al. (1994). Because the maximum wave load is associated to the maximum wave height; the input parameters for these methods have been taken to be the maximum wave height registered in the laboratory time series, and its associated wave period. While Sainflou (1928), Nagai (1973) and linear wave theory have been applied to regular and irregular waves, Takahashi et al. (1994) has been used only for irregular waves. We are aware of the fact that some of these formulas are being applied out of their range, but other than physical modelling they are the only tool available for the considered typologies.

Table 4 and Fig. 9 present the comparison between numerical and semi-empirical results. We can conclude that COBRAS-UC predicts wave loads better than most of the formulations used, the main reason being that the numerical model simulates the specific geometry of the vertical breakwater tested in the laboratory, while, for example, Sainflou is valid for vertical walls without rubble mound foundations.

Even if some of the methods result in mean errors of the same order, the main difference between the numerical and other methods can be found in the standard deviation which is much lower for the numerical model results.

Regarding rubble-mound breakwaters with crown walls, the formulations used in this work were the ones proposed by the CEM (USACE, 2002) and the PROVERBS (Probabilistic Design Methods for Vertical Breakwaters) (Oumeraci et al., 2001)

Pedersen (1996) formulation provides the horizontal wave force per running meter on the wall corresponding to 0.1% exceedance probability. The wave generated turning moment by the horizontal force is also provided. The wave uplift force can also be estimated by a simple approximation of a triangular shape law underneath the concrete cap. It is important to point out that the formulations presented by Pedersen (1996) obey a statistical fitting to experimental results, in which waves do no break in front of the structure.

Martín et al. (1999) presents a more sophisticated method. This formulation considers the existence of two force sources according to the physical processes involved in the wave generated loads, and it is suitable to be applied when broken waves reach the crown wall. Martín et al. (1999) distinguishes between dynamic pressure (generated during the abrupt change of direction of the bore front due to the crown wall) and reflecting pressure (effect which occurs after the instant of maximum run-up and is related to the water mass down-rushing the wall). In both cases, a pressure distribution along the crown wall can be calculated. By integrating these laws, the horizontal and uplift forces, and the corresponding moment can be estimated, identifying the worst scenario in terms of the concrete

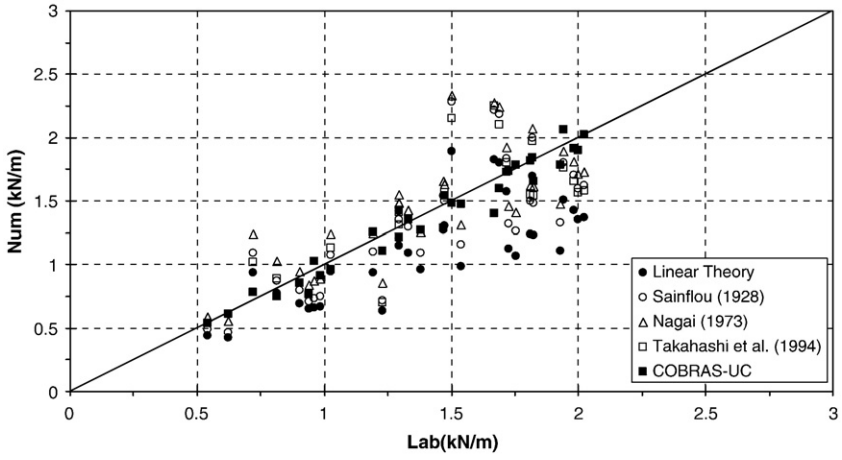


**Fig. 9.** Wave loads comparison with laboratory results. Regular and Irregular wave tests.

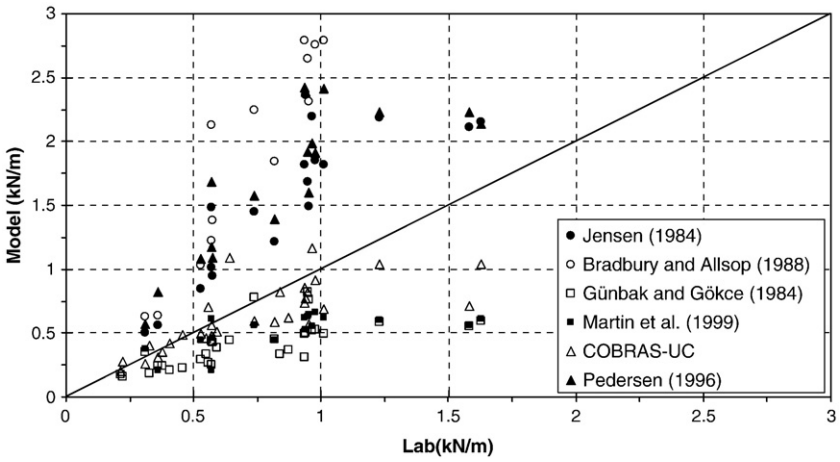


**Fig. 10.** Maximum horizontal wave loads comparison: Semi-empirical formulations.

crown wall stability. Additional formulations were also developed by Jensen (1984), Bradbury and Allsop (1988) and Günbak and Gökce (1984).

Fig. 10 and Table 5 summarize the comparison between semi-empirical horizontal wave load results based on laboratory measurements and numerical results. Because the maximum wave load is associated to the maximum wave height, Günbak and Gökce (1984) and Martín et al. (1999) have been applied considering the maximum wave height registered in the laboratory during complete time series and its associated wave period. Results obtained for Pedersen (1996), Jensen (1984) and Bradbury and Allsop (1988) are compared with the maximum wave load, because due to the number of simulated waves (100–200 waves) the maximum load registered is equivalent to the wave load, which is exceeded only 0.1% of the time.

Considering all the obtained results, we can conclude that there is significant dispersion in horizontal wave load prediction. This is probably due to the fact that wave load prediction on a crown wall is difficult, mainly because many wave process are involved: wave breaking, dissipation, turbulence, etc. and all of them are highly dependent of the breakwater geometry. According to Table 5 the closest agreement has been found between the COBRAS-UC and Martín et al. (1999) predictions. Again, it has to be pointed out that the better agreement achieved with COBRAS-UC was expected since the numerical simulation was carried out for the experimental geometry and input conditions.

In order to further investigate the model performance when simulating the mechanism of wave broken induced loads on a rubble mound structure, a detailed analysis has been carried out. Nine snapshots of the wave induced dynamic pressure distributions at the seaward face and underneath the crownwall are presented in Fig. 11. The dynamic pressure law along the crown wall is plotted using a solid line in each individual panel. Laboratory measurements are also represented using dots for the same time instants. In the lower panel, a wave profile in front of the breakwater, corresponding to gauge 10 (see lower panel in Fig. 1) is presented. The nine time instants along the wave time series are also represented using dots along the wave profile.

The wave induced pressure sequence described by Martín et al. (1999) is clearly seen in the nine displayed panels. In the first panel ($t=71.5$ s), the pressure law is observed to be affected by the wave trough which is inducing a negative dynamic pressure as can be seen at the lower part of the seaward face. At $t=71.6$ s, the broken wave is starting to run-up the rubble mound slope. The snapshot at $t=71.7$ s represents the dynamic pressure stage, as said before, generated during the abrupt change of direction of the bore front due to the crown wall. Both the numerical and experimental distributions show an almost uniform distribution along the seaward face. At $t=71.8$ s the maximum run-up is observed, yielding the reflected pressure stage described by Martín et al. (1999), which conforms a trapezoidal shape. In the rest of the snapshots, the trapezoidal shape is preserved, the pressure being reduced in magnitude according to the porous media drainage.

## 6. Full scale application

In this section the model will be used to evaluate the wave induced forces on two different structures at the prototype scale, a vertical breakwater and a rubble-mound breakwater. The goal of this section is to prove the ability and the potential of the model as a designing tool. The numerical setup at prototype scale has been considered based on the rules of thumb used in the laboratory scale simulations for validation. For example, the number of cells per wave length or per wave height has been kept constant, yielding a cell size around 20 cm × 40 cm close to the structures. Based on these assumptions, the computational cost is still competitive enough when a sea state of 3600 s is simulated using a standard PC, taking between 36 and 48 PC-hours for the cases presented in this work for both typologies.

Fig. 12 shows a vertical breakwater cross-section at Gijon's harbour extension. Wave attack characteristics are given by the following parameters: $H_s=9.0$ m, $H_{max}=14.2$ m $T_p=18.65$ s and SWL = +4.0 m. A 1 h sea state including 230 waves has been simulated on a numerical domain 1000 m long and 53 m high. The mesh resolution at the structure has been 0.5 m in the x-direction and 0.25 m in the y-direction. The rubble-mound layers underneath the caisson have been defined using the porous flow parameters proposed by (Lara et al., 2008).

The wave induced forces and moments analysis has been carried out following the methodology explained for the laboratory test simulations. Numerical results are compared with Takahashi et al. (1994) which gives the best results at the small scale.

**Table 5**
Horizontal loads: semi-empirical formulations and numerical model — rubble mound breakwater.

| Model | Mean error | Standard deviation |
|---|---|---|
| Jensen (1984) | +92.6% | ±32.8% |
| Bradbury and Allsop (1988) | +181.4% | ±67.3% |
| Pedersen (1996) | +65.7% | ±43.6% |
| Günbak and Gökce (1984) | −32.9% | ±14.% |
| Martín et al. (1999) | −22% | ±14.2% |
| Cobras-UC | −12.18% | ±21.17% |

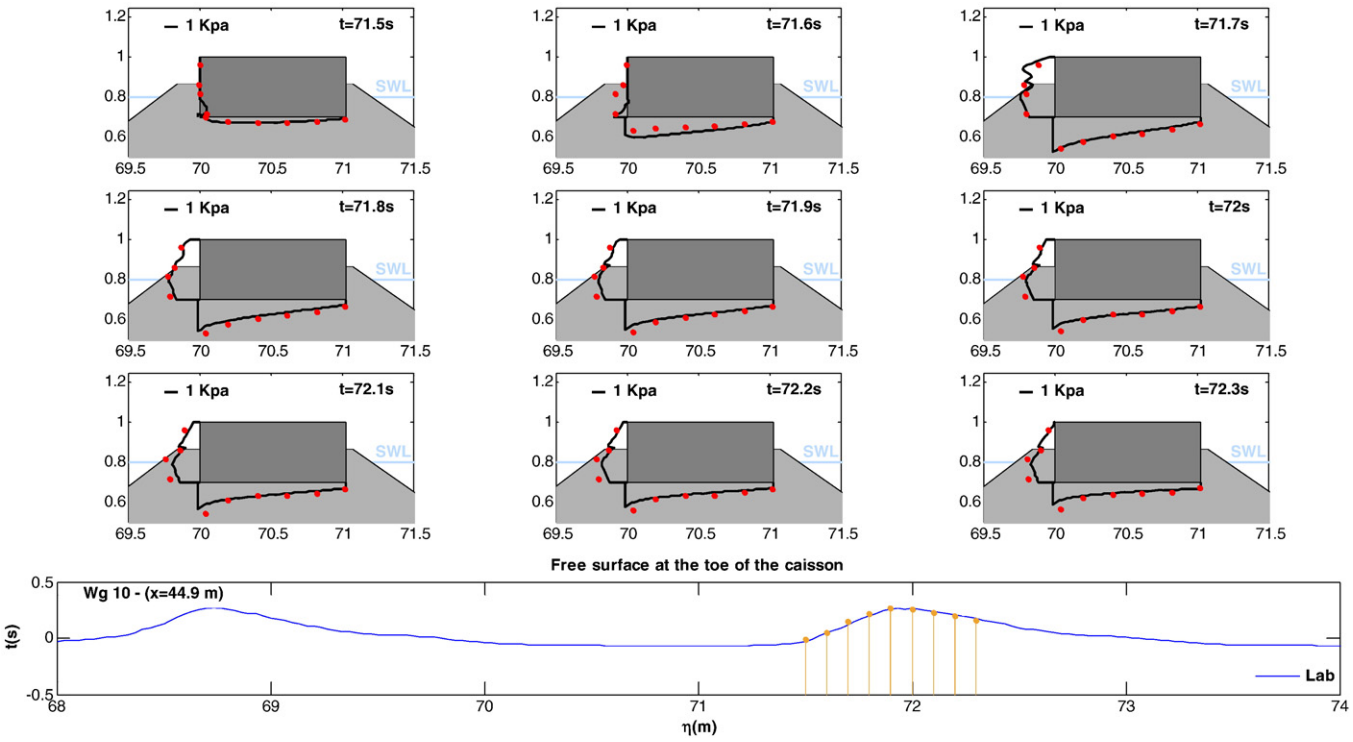


**Fig. 11.** Wave induced load mechanism by a broken wave. Case $H_s = 0.21$ m and $T_p = 3$ s. Nine snapshots: dynamic pressure laws (dots: laboratory results. solid line: numerical results). Lower panel: free surface elevation in front of the structure (dots: time instant corresponding to the nine displayed panels).

Fig. 13 shows the free surface in front of the breakwater (upper panel), horizontal and uplift force time histories (middle panels) for the studied sea state. The pressure distribution for the largest horizontal load in the record is also presented in the lower panel. The corresponding pressure distribution based on Takahashi et al. (1994) formulation (dotted line) is plotted together with the numerical results (solid line). Semi-empirical results have been calculated using the maximum incident wave recorded at the breakwater.

Comparative pressure distribution results show a very good agreement between the numerical model and Takahashi et al. (1994) formulation. Both predict the maximum pressure on the vertical face of the breakwater at the still water level. However, some discrepancies are observed at the lower and upper part of the vertical wall and also at the most onshore region underneath the structure. COBRAS-UC predicts the maximum wave load during the flow deceleration due to the wave-caisson interaction. At that moment, the wave induced flow changes from a mainly horizontal to a vertical motion. However Takahashi et al. (1994) formulation predicts the maximum wave pressure at the larger wave run-up instant. The differences observed at the lower part of the vertical wall, are because Takahashi et al. (1994) formulation does not consider the presence of a submerged berm to protect the caisson toe. The model results show a pressure decrement due to the energy damping within the berm. Discrepancies at the most onshore region underneath the structure are also due to the fact that the formulation application scenario implies that the still water level is the same on both sides of the breakwater, with no wave transmission effects, yielding a triangular uplift load distribution with a zero dynamic pressure value at the most onshore part. However, the presence of a quarry wall onshore the studied caisson increases the uplift loads, not included in the

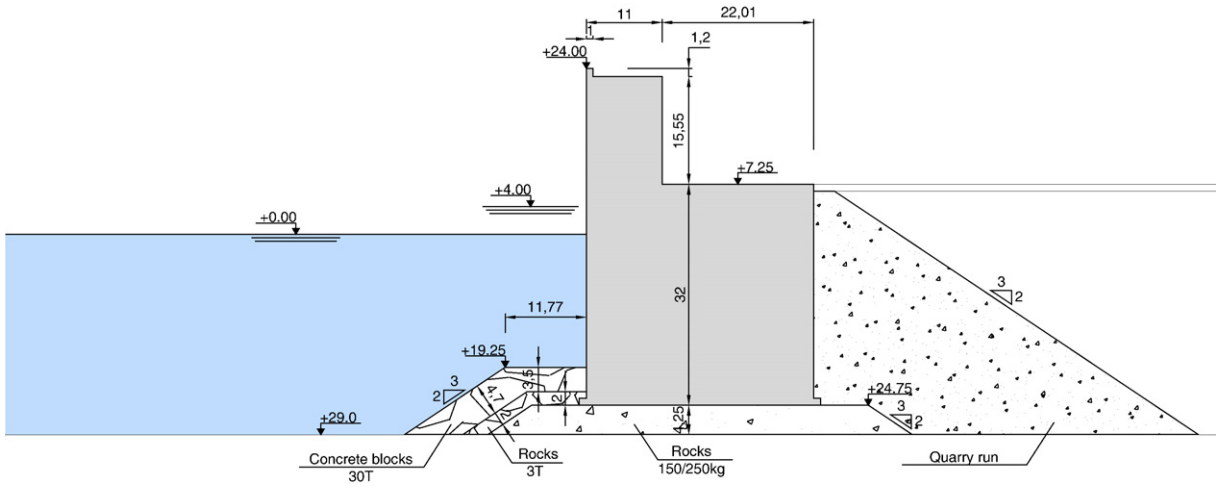


**Fig. 12.** Vertical breakwater cross-section at Gijon's Harbour extension (Spain).

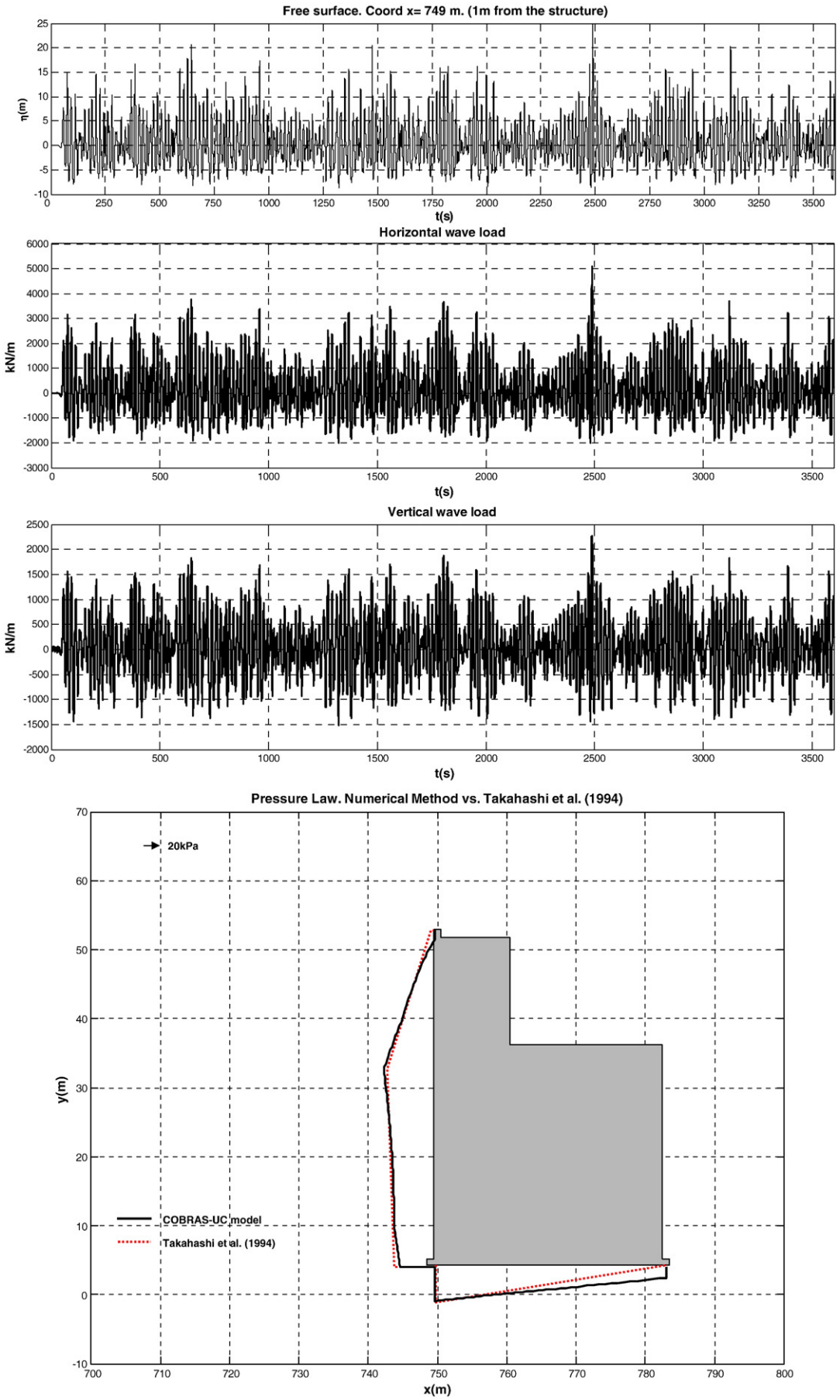


**Fig. 13.** Free surface, horizontal and vertical load time series. Maximum horizontal load pressure distribution (Numerical and Takahashi et al. (1994) results).

**Table 6**
Comparison between COBRAS-UC and Takahashi et al. (1994).

| Model | Horizontal forces (kN/m) | Vertical forces (kN/m) |
|---|---|---|
| COBRAS-UC | 5108 | 2155 |
| Takahashi et al. (1994) | 5037 | 1997 |
| Relative differences (COBRAS-UC vs Takahashi et al. (1994)) | +1.4% | +7.9% |

**Table 7**
Studies cases for the Laredo breakwater.

| Cases | Peak period $T_p$(s) | Significant wave height $H_s$ (m) |
|---|---|---|
| E1 | 15 | 8 |
| E2 | 15 | 10.7 |
| E3 | 18 | 6 |
| E4 | 18 | 8 |
| E5 | 18 | 10 |
| E6 | 20 | 6 |
| E7 | 20 | 8 |

Takahashi et al. (1994) formulation. The predicted law is trapezoidal, yielding an underestimation of the uplift forces if Takahashi et al. (1994) formulation is used. The discrepancies observed are a good example to show potential applications of the numerical model as a designing tool, when the formulations are outside of the applicability range.

Differences between the numerical and empirical resulting horizontal and vertical forces are presented in Table 6. As can be seen, minor differences exist with the numerical model predicting slightly higher resulting forces.

The second full scale application corresponds to the new port of Laredo breakwater. The port of Laredo is located on the northern coast of Spain and is to be protected by a rubble mound breakwater armoured with 60 ton concrete cubic blocks disposed in two layers (see Fig. 14). The breakwater under layer is made of two layers of 6 ton concrete cubic blocks and 300–1000 kg, respectively. The breakwater core consists of quarry run. On the landward side, a 750–1000 kg outer layer is placed on 250–500 kg rocks. The seaward side slope is 1/2 and the leeward side is 3/2. The tidal range considered for this study is 5.30 m from the reference level. The water depth at the breakwater toe is −9.00 m, from the reference level, so the total water depth in front of the structure is 14.3 m. On the breakwater crest, a crown-wall is placed with an 8.34 m-long service road enabling access to the breakwater. The crown wall crest is at +17.00 m from the reference level. On the seaward face of the crown-wall, a nose is placed in order to reduce wave overtopping. The crown-wall foundation is at +5.50 m.

The model applicability has been tested with wave conditions presented in Table 7. Numerical results are compared against Pedersen (1996) and Martín et al. (1999) formulations.

The numerical calculations were performed in a 1000 m long and 45 m high numerical flume. A non uniform grid was considered, using a finer resolution around the breakwater crown wall of 0.40 m ($H$) by 0.20 m ($V$). In order to take into account the varying depth of the bathymetry in front of the breakwater, a uniform 1/100 slope was used in the numerical test. The simulations were 3600 s long, including between 238 and 363 waves, depending on the case. Synthetic wave series were created based on a TMA-type spectrum, ensuring the location of the maximum wave height around the time 1000 s. Moreover, the ratios $H_{max}/H_s$ and $\eta_{max}/H_{max}$ were forced to be at least 1.8 and 0.5, respectively. Porous media parameters considered for the simulations were those proposed by Losada et al. (2008).

Comparative results for the Pedersen (1996) and Martín et al. (1999) method and the COBRAS-UC model are presented in Fig. 15. Comparisons for wave induced horizontal and uplift forces are presented in the top left panel and top right panel, respectively. The moments due to both forces are presented in the lower panels. Force and moment values have been represented in a non-dimensional form, based on the incident wave characteristics, in order to directly compare the different results. The numerical model results correspond to the maximum horizontal and uplift force and moment of the whole simulation.

From the comparison, it can be observed that Pedersen (1996) shows larger values for both the horizontal and vertical forces than Martín et al. (1999) and the numerical model. Pedersen (1996) does not consider breaking waves in front of the structure and overestimates the wave-induced forces. Martín et al. (1999) and the numerical model show very close values for the horizontal forces, but larger differences are observed for the uplift loads. The source of the difference can be found in the prediction of the wave run-up over the external armour layer. While Martín et al. (1999) follows the formulation introduced by Losada and Gimenez-Curto (1981) which partially takes into account wave breaking, the model solves the wave field in front of the structure, reproducing the wave run-up. This fact is more clearly visible in the moment calculation, where the shape and the magnitude of the pressure distribution underneath the breakwater crown wall are different.

Fig. 16 presents additional information obtained from the numerical model that can be useful for stability analysis. In the upper panel, the free surface time series for case 5 (see Table 7) is presented. The second and third panels present the sliding and overturning sliding safety coefficient for the complete time series. The time of the minimum safety coefficients and its magnitude can be

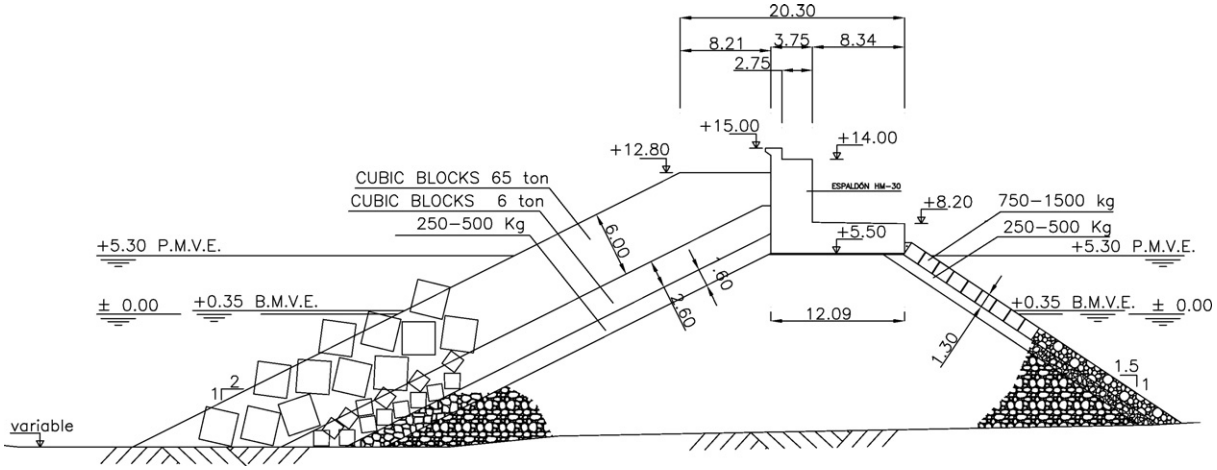


**Fig. 14.** Laredo breakwater cross-section.

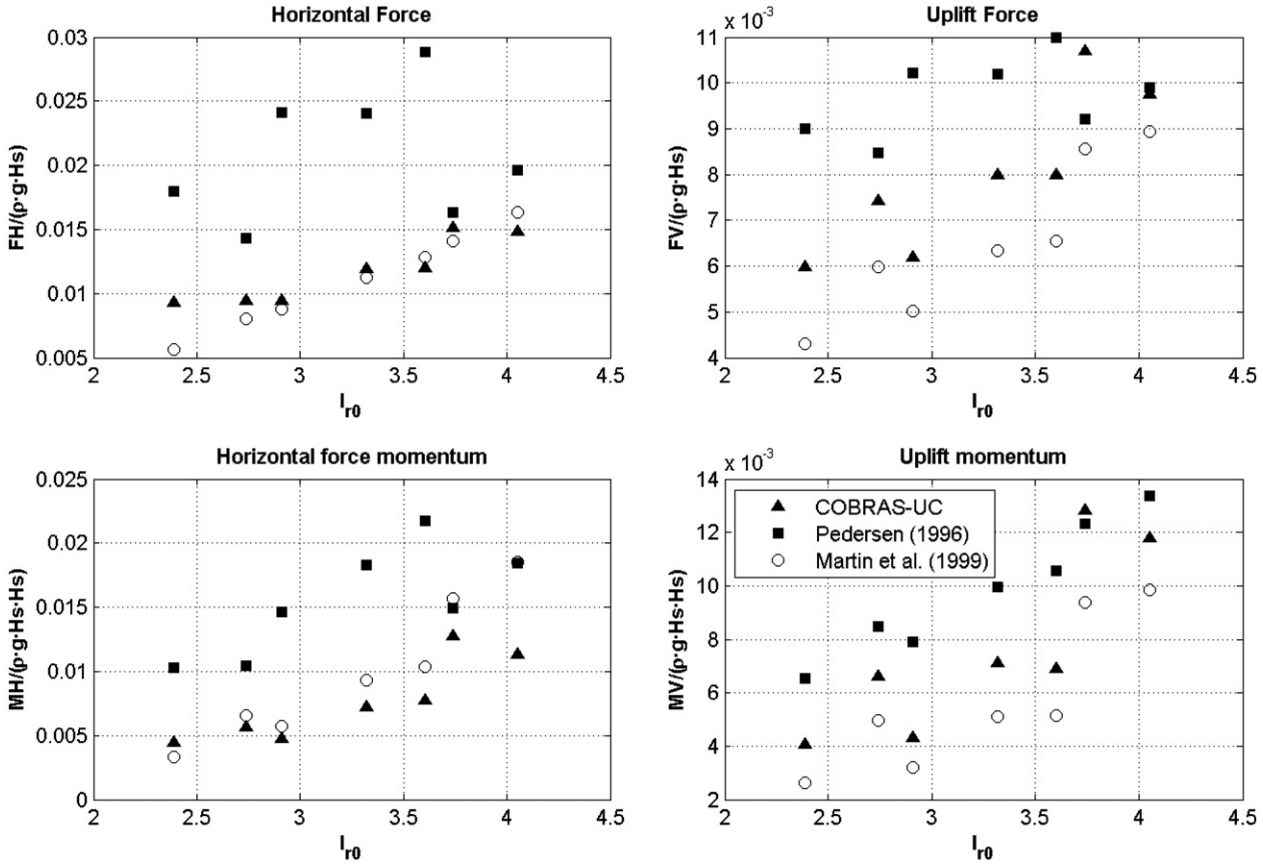


**Fig. 15.** Comparative results of wave induced horizontal forces (top left panel), uplift forces (top right panel), horizontal momentum (bottom left panel) and uplift force momentum (bottom right panel), for the Pedersen (1996) and Martín et al. (1999) method and the COBRAS-UC model.

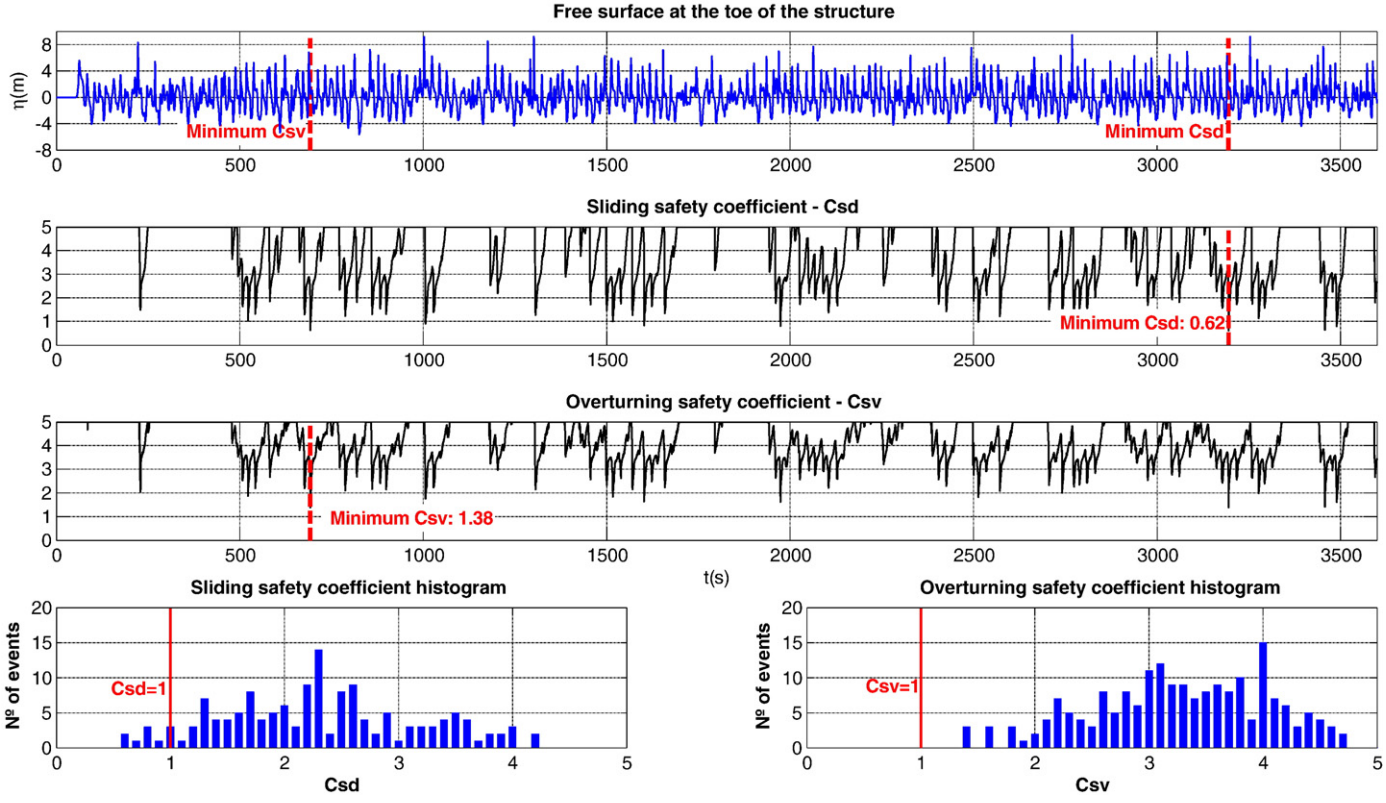


**Fig. 16.** Sliding and overturning safety coefficient time series and histograms for case 5.

calculated. A histogram of sliding safety coefficients can be obtained to evaluate the probability of exceeding a given threshold of the safety coefficients.

## 7. Conclusions

In this work, we have analyzed the ability of a two-dimensional numerical model based on the RANS equations, named COBRAS-UC, to address the wave induced loads on coastal structures. The model can simulate free surface, wave pressure, velocities, turbulence, and dissipation due to breaking and porous flow, making it appropriate to consider wave interaction with several kinds of structure typologies. The model has been tested for a vertical coastal structure on a low-mound and for a rubble mound breakwater including a crown-wall. In the first part of the paper, numerical results are compared with experimental records obtained on a 1:20 physical model scale. Numerical results of pressure, forces and moments are also compared with existing semi-empirical or theoretical formulations for coastal structure stability. COBRAS-UC shows an excellent performance for vertical structures with differences between numerical and measured values less than 5%. Even if some of the other formulations used are able to reach similar orders of error, dispersion in the results is much lower for the numerical model.

For the rubble mound breakwater case, differences increase for both the numerical and semi-empirical formulations, due to the higher complexity in simulating the relevant processes involved. Still COBRAS-UC performs quite well with results equivalent to Martín et al. (1999).

In order to analyze the possible application of the model to real cases, two applications for prototype cross-sections and real wave conditions are presented. Results have been successfully compared with semi-empirical formulations, using reasonable simulation times for an entire simulated sea state. The model has been proven to be useful to overcome some limitations inherent to the formulations. The methodology presented based on the application of COBRAS-UC may complete the approach based on currently existing methods and tools.

## 8. Discussion

In this work, a two dimensional model has been used as a tool to study wave-structure interaction. The model has been presented to work as a numerical flume to study wave loads for any type of conventional or non-conventional structures, and on laboratory scales as well as at prototype scales. There is no limitation for structure geometries or wave characteristics. Any type of structure can be simulated: permeable or impermeable, submerged or emerged, single-layered or multi-layered, etc, for several wave characteristics, regular or irregular waves or linear or non-linear waves subject to the assessment of porous parameters.

To date, models based on two-dimensional RANS approximations are possibly the best suited to study wave and structure interaction for engineering purposes, since computational efforts (48 h for 100 waves in a conventional PC) are reasonable and the number of simplifying assumptions is considerably reduced, compared to other approaches. The accuracy of the solutions has been proven to be around 15% in the worst scenario, which reveal the applicability of the model to design.

In our opinion, the use of this model can overcome the limitations of those physical tests which do not fully represent the wave structure interaction process and of those formulations with a narrow range of applicability. The use of the model represents a tailored design wave flume for each individual problem, opening the possibility to carry out a sensibility analysis of the geometrical parameters or the influence of the porous media properties on the hydrodynamic response of the structure, with no limitations regarding the number of time series gauge locations. Moreover, there are no limitations on the wave generation and the active wave absorption is also considered in the model. The analysis of wave overtopping carried out in Losada et al. (2008) and Lara et al. (2008) and the wave induced load analysis covered in the present work have shown that COBRAS-UC has a high potential to become a complementary tool to analyze the hydraulic response of structures.

On the other hand, the model has some limitations regarding several of the physical processes which the model does not consider in the equations. Processes such as impulsive forces, in which the two phase flow plays an important role, or the three dimensional effects on coastal structures cannot be considered by the present version of the model.

## Acknowledgments

The authors thankfully acknowledge the computer resources, technical expertise and assistance provided by the Spanish Supercomputing Network (RES) node at Universidad de Cantabria. J.L. Lara is indebted to the M.E.C. for the funding provided in the Ramon y Cajal Program.

## References

Bradbury, A.P., Allsop, N.W., 1988. Hydraulic effects of breakwater crown walls. Proceedings of the Breakwaters '88 Conference, Institution of Civil Engineers. Thomas Telford Publishing, London, UK, pp. 385–396.
Brocchini, M., Dodd, N., 2008. Nonlinear shallow water equation modeling for coastal engineering. Journal of Waterway Port Coastal and Ocean Engineering 134 (2), 104.
Engsig-Karup, A.P., Hesthaven, J.S., Bingham, H.B., Warburton, T., 2008. DG-FEM solution for nonlinear wave-structure interaction using Boussinesq-type equations. Coastal Engineering 55 (3), 197–208.
Garcia, N., Lara, J.L., Losada, I.J., 2004. 2-D numerical analysis of near-field flow at low-crested permeable breakwaters. Coastal Engineering 51, 991–1020.
Goda, Y., 1974. New wave pressure formulae for composite breakwaters. Proceedings of the 14th Conference of Coastal Engineering. ASCE, pp. 1702–1720.
Goda, Y., 1985. Random seas and design of maritime structures. University of Tokyo. ISBN 981023256X.
Günbak, A.R., Gökce, T., 1984. Wave screen stability of rubble mound breakwaters. Int. Symp. of Maritime Structure in the Mediterranean Sea. Athens, Greece, p. 2999-2112.
Hsu, T.-J., Sakakiyama, T., Liu, P.L.-F., 2002. A numerical model for wave motions and turbulence flows in front of a composite breakwater. Coastal Engineering 46, 25–50.
Hur, D., Mizutani, N., 2003. Numerical estimation of the wave forces acting on a three-dimensional body on submerged breakwater. Coastal Engineering 47 (3), 329–345.
Jensen, O.J., 1984. A Monograph on Rubble Mound Breakwaters. Danish Hydraulic Institute, Denmark.
Lara, J.L., Garcia, N., Losada, I.J., 2006a. RANS modelling applied to random wave interaction with submerged permeable structures. Coastal Engineering 53, 395–417.
Lara, J.L., Losada, I.J., Liu, P.L.-F., 2006b. Breaking waves over a mild gravel slope: experimental and numerical analysis. Journal of Geophysical Research, AGU 111, C11019. doi:10-1029/2005 JC003374.
Lara, J.L., Losada, I.J., Guanche, R., 2008. Wave interaction with low mound breakwaters using a RANS model. Ocean engineering 35, 1388–1400. doi:10.1016/j.oceaneng.2008.05.006.
Li, T., Troch, P., De Rouck, J., 2004. Wave overtopping over a sea dike. Journal of Computational Physics 198 (2), 686–726.
Liu, P.L.-F., Hsu, T.-J., Lin, P., Losada, I.J., Vidal, C., Sakakiyama, T., 1999. The Cornell breaking wave and structure (COBRAS) model. Proceedings of the International Conference Coastal Structures'99, Santander, Spain, pp. 169–174.
Losada, M.A., Gimenez-Curto, L.A., 1981. Flow characteristics on rough, permeable slopes under wave action. Coastal Engineering, vol. 4. Elsevier, pp. 187–206.
Losada, I.J., Dalrymple, R.A., Losada, M.A., 1993. Water waves on crowned breakwaters. Journal of Waterways, Port, Coastal and Ocean Engineering, ASCE 119 (4), 367–380.
Losada, I.J., Lara, J.L., Damgaard, E., Garcia, N., 2005. Modelling of velocity and turbulence fields around and within low-crested rubble-mound breakwaters. Coastal Engineering 52, 887–913.
Losada, I.J., Lara, J.L., Guanche, R., Gonzalez-Ondina, J.M., 2008. Numerical analysis of wave overtopping of rubble mound breakwaters. Coastal Engineering 55 (1), 47–62.
Martín, F.L., Losada, M.A., Medina, R., 1999. Wave loads on rubble mound breakwater crown walls. Coastal Engineering 37, 149–174.
Nagai, S., 1973. Wave forces on structures. Advances in Hydroscience, vol. 9. Academic Press Press, New York, pp. 253–324.
Oumeraci, H., et al., 2001. Probabilistic Design Tools for Vertical Breakwaters (PROVERBS). A.A. Balkema Publishers, 373pp.
Pedersen, J., 1996. Experimental study of wave forces and wave overtopping on breakwater crown walls. Series paper 12, Hydraulics & Coastal Engineering Laboratory, Department of Civil Engineering, Aalborg University, Denmark.

Sainflou, M., 1928. Essai sur les digues maritimes verticals. Annals des Ponts et Chaussee 98 (9).
Takahashi, S., Tanimoto, K., Shimosako, K., 1994. A proposal of impulsive pressure coefficient for design of composite breakwaters. Proceedings of the International Conference on Hydro-Technical Engineering for Port and Harbor Construction. Port and Harbour Research Institute, Yokosuka, Japan, pp. 489–504.
Torres-Freyermuth, A., Losada, I.J., Lara, J.L., 2007. Modeling of surf zone processes on a natural beach using Reynolds-averaged Navier–Stokes equations. Journal of Geophysical Research 112, C09014. doi:10.1029/2006JC004050.
U.S. Army Corps of Engineers, 2002. Coastal Engineering Manual (CEM). Engineer Manual 1110-2-1100. U.S. Army Corps of Engineeris, Washington, D.C. (in 6 volumes).